A Hip-Knee Joint Coordination Evaluation System in Hemiplegic Individuals Based on Cyclogram Analysis

Ningcun Xu[1], Chen Wang[2], Liang Peng[2(✉)], Jingyao Chen[1], Zhi Cheng[1], Zeng-Guang Hou[1,2(✉)], Pu Zhang[3], and Zejia He[3]

[1] Macau University of Science and Technology, Macao 999078, China
2202853NMI30001@student.must.edu.mo
[2] State Key Laboratory of Multimodal Artificial Intelligence Systems, Institute of Automation, Chinese Academy of Sciences, Beijing 100190, China
{liang.peng,zengguang.hou}@ia.ac.cn
[3] Beijing Bóai Hospital, China Rehabilitation Research Center, Beijing 100068, China

Abstract. Inter-joint coordination analysis can provide deep insights into assessing patients' walking ability. This paper developed a hip-knee joint coordination assessment system. Firstly, we introduced a hip-knee joint cyclogram generation model that takes into account walking speed. This model serves as a reference template for identifying abnormal patterns in the hip-knee joints when walking at different speeds. Secondly, we developed a portable motion capture platform based on stereovision technology. It uses near-infrared cameras and markers to accurately capture kinematic data of the human lower limb. Thirdly, we designed a hip-knee joint coordination assessment metric DTW-ED (Dynamic Time Wrapping - Euclidean Distance), which can score the subject's hip-knee joint coordination. Experimental results indicate that the hip-knee joint cyclogram generation model has an error range of $[0.78^\circ, 1.08^\circ]$. We conducted walking experiments with five hemiplegic subjects and five healthy subjects. The evaluation system successfully scored the hip-knee joint coordination of patients, allowing us to differentiate between healthy individuals and hemiplegic patients. This assessment system can also be used to distinguish between the affected and unaffected sides of hemiplegic subjects. In conclusion, the hip-knee joint coordination assessment system developed in this paper has significant potential for clinical disease diagnosis.

Keywords: Hip-Knee Cyclogram · Joint Coordination Evaluation Metric · B-spline Curve · Motion Capture System · Stereo Vision · Dynamic Time Warping

This work was supported in part by the National Key Research and Development Program of China under Grant 2022YFC3601200; in part by the National Natural Science Foundation of China under Grant 62203441 and Grant U21A20479, and in part by the Beijing Natural Science Foundation under Grant L222013.

B. Luo et al. (Eds.): ICONIP 2023, LNCS 14449, pp. 589–601, 2024.
https://doi.org/10.1007/978-981-99-8067-3_44

1 Introduction

Gait analysis is a valuable tool that systematically differentiates human walking patterns. It finds applications in various fields, including diagnosing the health status of patients with gait disorders for clinicians [1], providing comprehensive evaluations of the effects of surgery or lower limb rehabilitation aids on patients [2,3], aiding professional athletes in correcting their movement posture [4], and assessing the fall risk among the elderly [5], and more.

Traditionally, clinicians have conducted gait analysis by using motor ability evaluation scales, such as the Brunnstrom Recovery Stage (BRS) [6] and the Fugl-Meyer assessment (FMA) [7]. However, the assessment results depend heavily on the experience level of clinicians.

Cyclogram, also known as angle-angle plot, is a very useful technology to describe inter-joint coordination, which was first proposed by Grieve et al. [8]. Compared with the redundant gait parameters in the gait report, the cyclogram can capture the subtle variability of gait patterns during walking and provide a more insightful analysis of the abnormal gait.

Researchers have proposed many metrics to qualitatively and quantitatively evaluate the inter-joint coordination based on cyclogram. Goswami et al. [9] designed the hip-knee joint coordination evaluation metric "cyclogram moments" by taking the geometric moments of the cyclogram as the descriptor of the inter-joint coordination. Another cyclogram-based metric is vector coding [10], which was defined as the "coupling angle" between two adjacent points on the cyclogram [11]. In order to better understand the changes in the gait patterns, Chang et al. [12] divided the coupling angle into four bins named in-phase, anti-phase, rear-foot phase, and fore-foot phase. Needham et al. [13] also separated the coupling angle into four bins: in-phase with proximal dominance, in-phase with distal dominance, anti-phase with proximal dominance, and anti-phase with distal dominance. The improved vector coding techniques were called "coupling angle binning" or "phase binning" by Beitter et al. [14]. They proposed a more comprehensive binning-based metric by combining the previous two metrics.

In this paper, we developed an active lower limb motion capture system based on stereo vision technology to collect the walking kinematics data of the subjects. A hip-knee cyclogram generation model related to walking speed was designed by using the B-spline curve. The model's parameters are transparent and interpretable. The hip-knee cyclogram produced by the generation model can be used as the reference template for the hip-knee joint coordination analysis. We also proposed the hip-knee joint coordination assessment metric DTW-ED (Dynamic Time Wrapping - Euclidean Distance), which can score the subject's hip-knee joint coordination and distinguish between healthy individuals and hemiplegic patients. Compared with the existing gait analysis tools, the advantages of the evaluation system proposed by this paper are its low cost, high mobility, and convenient deployment.

2 Hip-Knee Joint Coordination Assessment System

2.1 Lower Limbs Motion Capture Platform

System Composition. In this study, an active lower limbs motion capture platform was developed to collect the kinematics data of hip and knee joints during walking. As shown in Fig. 1, the motion capture platform is used in a hand-held way for the moving scene, which mainly consists of a near-infrared binocular camera, an infrared light source, an RGB camera, a palm-sized computer, some magic cable ties, and passive reflective ball markers.

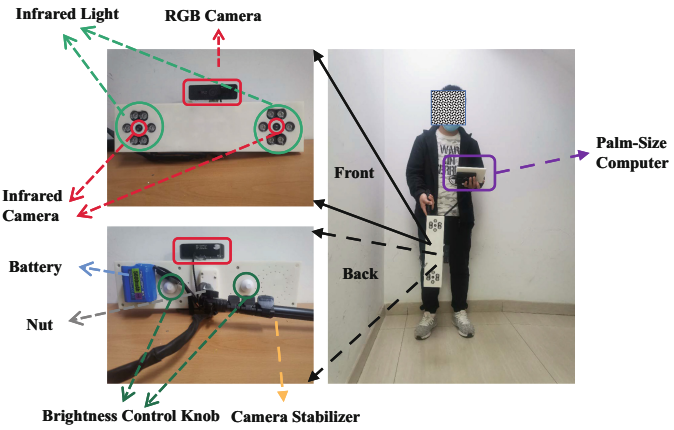

Fig. 1. Lower limbs motion capture platform in a hand-held way for mobile scene.

Hip and Knee Joint Angles Calculation. Firstly, the definitions of the hip and knee joints angle are illustrated in Fig. 2. The hip joint angle θ_{hip} was defined as the intersection angle of the body gravity vector relative to the connection line L_6 between marker M_1 and marker M_2. The knee angle θ_{knee} was the intersection angle of the extended line of L_6 relative to the connection line L_7 between reflective ball marker M_2 and marker M_3 [15]. In the walking experiment, these markers were placed bilaterally in the centerline of the thigh, the flexion-extension axis of the knee joint, and the lateral malleolus of the ankle joint [16].

Then, as shown in Fig. 3, the main steps of calculating the hip and knee joint angle include extracting frames from recording an individual's walking video, correcting frames based on the parameters of the binocular camera, detecting the reflective ball markers, matching the corresponding pixel points, calculating the position of markers based on stereo vision technology, and calculating the hip and knee joint angle.

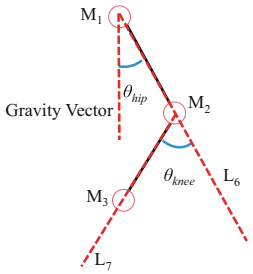

Fig. 2. Definitions of hip and knee joint angle in the sagittal plane.

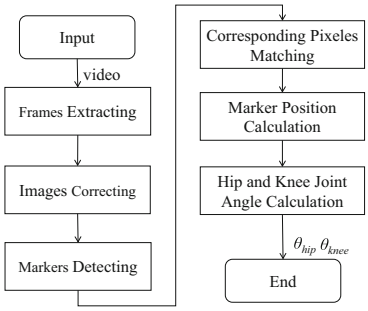

Fig. 3. Flow chart for calculating the hip and knee joint angle from recording human lower limbs motion video.

2.2 Hip-Knee Cyclogram Generation Model

Walking Biomechanics Dataset. WBDS is the largest public gait dataset, which was made by Claudiane et al. [17]. It comprehensively considers the effects of the walking environment, age, and gait speed on gait patterns.

We use the hip and knee joint kinematics data in the sagittal plane from 24 healthy young volunteers walking on the treadmill to establish the hip-knee cyclogram generation model. The eight walking speeds in the treadmill trials are denoted as Speed1-Speed8, respectively.

B-Spline Curve. The spline curve is a continuous and smooth curve generated by a set of control points. The spline curve is divided into two types: the interpolation spline curve and the approximation spline curve. The former passes through the control points, while the latter does not. Therefore, we used the B-spline curve to establish the hip-knee cyclogram generation model. The definition of the B-spline curve is that

$$\mathbf{C}(u) = \sum_{i=0}^{n} N_{i,k}(u)\mathbf{cp}_i, u \in [0,1], \tag{1}$$

where, the two-dimensional vector $\mathbf{C}(u)$ represents the generating B-spline curve over the parameter u. The range of the parameter u is [0, 1]. We denote the $n+1$ control points as CP_0, CP_1, CP_2, . . . , CP_n, and the vector $\mathbf{cp}_i$ is the coordinate of the i-th control point. The $N_{i,k}(u)$ is the basis function of the k-degree B-spline curve, which is over the parameter u.

The basis function $N_{i,k}(u)$ can be calculated by using the Cox-deBoor algorithm in recursive way, as shown in (2) [18].

$$\begin{cases} N_{i,0}(u) = \begin{cases} 1, \&if\ t_i \le u \le t_{i+1} \\ 0, \&other \end{cases} \\ N_{i,k}(u) = \dfrac{(u-t_i)N_{i,k-1}(u)}{t_{i+k}-t_i} + \\ \qquad \dfrac{(t_{i+k+1}-u)N_{i+1,k-1}(u)}{t_{i+k+1}-t_{i+1}} \qquad t_i \le u \le t_{i+1}, k \ge 1 \end{cases} \tag{2}$$

As shown in (2), when k is 0, the basis function $N_{i,0}(u)$ on the knot interval $[t_i,\ t_{i+1}]$ is constant 1; Otherwise, it is constant 0. And, when the degree $k \ge 1$, the basis functions $N_{i,k}(u)$ is calculated by the recursive formula. The t_i represents the knot value, and the $m+1$ knot values form the knot vector $\mathbf{t} = \{t_0, t_1, t_2, ..., t_m\}$, which can divide the value range of parameter u into different bins, i.e. $[t_i,\ t_{i+1}]$. Thus, $N_{i,k}(u)$ can determine the influence of control points on the curve shape.

Above all, the three foundational elements of the B-spline curve are the degree k, $n+1$ control points CP_0, CP_1, CP_2, . . ., CP_n and the knot vector $\mathbf{t}$. There are following relationship: $m = n+k+1$, among the three foundational elements [18].

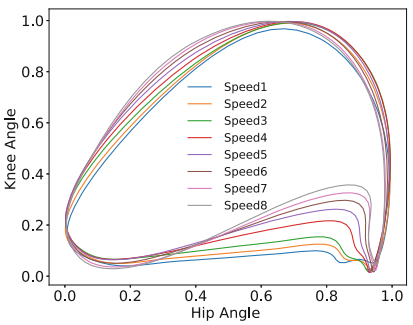

Fig. 4. The average hip-knee cyclograms from 24 healthy young subjects at each walking speed.

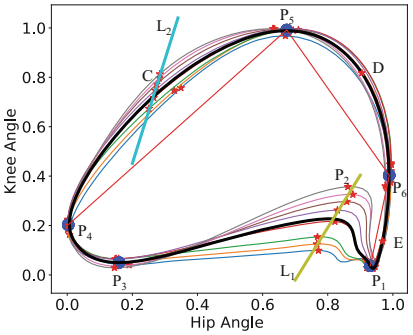

Fig. 5. Feature points of original hip-knee cyclograms.

Data Preprocess. The purpose of data preprocessing is to eliminate the amplitude difference of joint angle in different individuals and to extract general features on the hip-knee cyclograms of all volunteers. Firstly, all volunteers' hip joint angle and knee joint angle data were normalized, respectively. Secondly, we calculated the average hip-knee cyclogram of 24 healthy young volunteers at each walking speed, which was regarded as the original cyclograms, as shown in Fig. 4.

Feature Points. For determining the three foundational elements of the B-spline curve, we firstly extracted nine feature points and established their expression relative to walking speed s by analyzing the characteristic variety of the original hip-knee cyclograms at different walking speeds. Figure 5 shows nine feature points, P_1, P_2, P_3, P_4, P_5, P_6, C, D, E, on hip-knee cyclograms at the eight kinds of walking speeds. The black hip-knee cyclogram is the average curve of these cyclograms at all walking speeds. Feature points P_1, P_2, P_3, P_5 were located at the first valley, the first peak, the second valley, and the second peak of the knee joint angle curve, respectively. And the valley and the peak of the hip joint angle were defined as the feature points P_4 and P_6, separately. The feature point C was defined as the point farthest from the connection line between P_4 and P_5 on terminal stance and pre-swing phase of the hip-knee cyclogram. Feature points D and E were respectively defined as the points on the swing phase of the average angle cyclogram with the largest distance relative to the straight line between P_5 and P_6, and the straight line between P_6 and P_1.

In the next subsection, the nine feature points would be used to yield 12 control points of B-spline curve, and the Cox-deBoor algorithm would be used to generate the standard hip-knee cyclograms at different walking speeds.

Standard Hip-Knee Cyclogram Generating. Based on the nine feature points on hip-knee cyclograms, 12 control points of B-spline curve were defined as CP_i, i = 0, 1, 2, 3, 4, 5, 6, 7, 8, 9, 10, 11, as shown in Fig. 6.

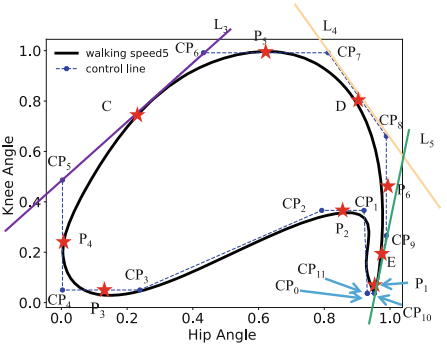

Fig. 6. Definitions of 12 control points. (Color figure online)

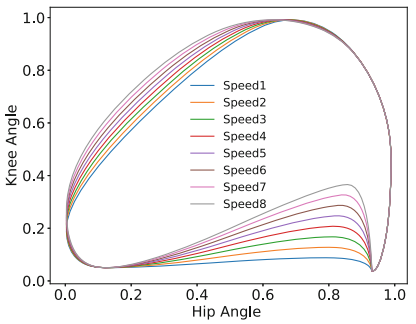

Fig. 7. The cyclograms produced by hip-knee cyclogram generating model at eight walking speeds.

The black curve represents the original hip-knee cyclogram at walking Speed5. The red stars represent the nine feature points. The blue circles represent the control points and the dotted lines represent the control line between two adjacent control points.

Control point CP_0 and control point CP_{11} were located at the feature point P_1 for generating the closed cyclogram. Control point CP_1 was defined as horizontal right of feature point P_2, the coordinate of which was [P_{1x} - 0.01, P_{2y}]. Control point CP_2 was defined as horizontal left of feature point P_2, the coordinate of which was [P_{2x} −0.09, P_{2y}]. Control point CP_3 was defined as the horizontal right of the feature point P_3, the coordinate of which was [P_{3x} + 0.08, P_{3y}]. The abscissa and ordinate of the control point CP_4 were respectively defined as the abscissa of the feature point P_4 and the ordinate of the feature point P_3, the coordinate of which was [P_{4x}, P_{3y}]. The control point CP_5 was defined as the intersection of the straight line $x = P_{4x}$ and the straight line L_3, which passed through point C and had the same slope as the connecting line between feature point P_4 and feature point P_5. The control point CP_6 was the intersection of the straight line $y = P_{5y}$ and the straight line L_3. The control point CP_7 was defined as the intersection of the straight line $y = P_{5y}$ and the straight line L_4, which passed through point D and had the same slope as the connecting line between feature point P_5 and feature point P_6. The control point CP_8 was defined as the intersection of the straight line $x = P_{6x}$ and the straight line L_4. The control point CP_9 was defined as the intersection of the straight line $x = P_{6x}$ and the straight line L_5, which passed through point E and had the same slope as the connecting line between feature point P_6 and feature point P_1.The control point CP_{10} was defined as the intersection of the straight line $y = P_{1y}$ and the straight line L_5.

Next, we used the cubic B-spline curve to establish the hip-knee cyclogram generation model, so that the order$k+1$ is 3. In light of the quantitative relationship between the three foundational elements of B-spline curve, $m = n + k + 1$, the number of knot values $m+1$ is 14. In order to generate a smooth and closed cyclogram, the knot vector $\mathbf{t}$ was defined as $\mathbf{t}$ = {0, 0, 0, 0.1, 0.2, 0.3, 0.4, 0.5, 0.6, 0.7, 0.8, 0.9, 1, 1, 1}.

The basis function $N_{i,k}(u)$ could be calculated by (2). Then, the hip-knee cyclogram can be generated by the formula (1), as shown in Fig. 7.

Above all, we indirectly established hip-knee cyclogram generation model related to walking speed s by using B-spline curve, which can produce the hip-knee cyclogram at some walking speed.

2.3 Hip-Knee Joint Coordination Assessment Metric

The hip-knee cyclograms of individuals with different severities of gait disorder have significant shape distinctions [15]. Clinicians can easily distinguish the walking ability of individuals by observing the shape features of their hip-knee cyclograms. Therefore, we regarded the hip-knee joint coordination evaluation of individuals as the shape similarity assessment of their hip-knee cyclograms relative to the standard cyclogram generated in former section.

We introduced a new metric called DTW-ED for evaluating hip-knee joint coordination. DTW-ED combines two key components: DTW-based corresponding points matching between the hip-knee cyclograms and ED-based mean

matching error calculation. The resulting assessment value is referred to as the hip-knee joint coordination assessment value, denoted as *dtw-ed*.

Suppose we have two sets of sample points represented as $\mathbf{A}$ and $\mathbf{B}$ on the cyclograms, both with dimensions of $n \times 2$. Here, $\mathbf{A}$ refers to the standard hip-knee cyclogram generated in Sect. 2.2, while $\mathbf{B}$ represents the hip-knee cyclogram of an individual at a specific walking speed. The DTW-ED metric takes these two cyclograms, $\mathbf{A}$ and $\mathbf{B}$, as inputs and provides the hip-knee joint coordination evaluation value, *dtw-ed*, as the output. The main calculation steps involve determining the distance matrix $\mathbf{D_{AB}}$, computing the cumulative cost matrix $\mathbf{C}_{dtw}$, finding the shortest path $\mathbf{P}_{path}$, and calculating the evaluation value *dtw-ed*. The shortest matching path $\mathbf{P}_{path}$, with dimensions of $n \times 2$, plays a fundamental role in the quantitative assessment metric. Visualizing this path on the cyclograms can aid clinicians in qualitatively assessing hip-knee joint coordination. The *dtw-ed* value is defined as the average Euclidean distance between corresponding points on the shortest path $\mathbf{P}_{path}$.

3 Experiment and Results Analysis

3.1 Hip-Knee Cyclogram Modeling Results

As shown in Fig. 7, the standard hip-knee cyclograms at different walking speeds were produced by the hip-knee cyclogram generation model. The results show the hip-knee cyclogram generation model can accurately describe the characteristic variety of the cyclogram at different walking speeds.

Next, we employed Dynamic Time Warping (DTW) to extract corresponding points between the cyclogram generated by the hip-knee cyclogram generation model and the original cyclogram at the corresponding walking speed. The model's Mean Absolute Difference (MAD) was defined as the average Euclidean distance among all corresponding points.

Table 1. Hip-Knee cyclogram modeling error results

Walking Speed	Speed1	Speed2	Speed3	Speed4
MAD/degree[a]	0.96 ± 0.6	0.78 ± 0.54	1.02 ± 0.6	0.9 ± 0.42
Walking Speed	Speed5	Speed6	Speed7	Speed8
MAD/degree	0.84 ± 0.42	0.72 ± 0.42	0.96 ± 0.54	1.08 ± 0.54

[a] MAD: mean absolution difference

After inverse normalization, the modeling errors at different walking speeds are given in Table 1. The range of the modeling errors is $[0.72°, 1.08°]$[1]. Thus, the modeling errors are small enough. Figure 8 visualize the standard hip-knee cyclogram and the original hip-knee cyclogram at the walking speed8. The black stars

[1] The coefficient of inverse normalization was set as $60°$.

represent the cyclogram produced by the hip-knee cyclogram generation model. The red circles represent the original cyclogram. The black lines represent the connection line of corresponding points. It can be seen that the hip-knee cyclogram generated by the hip-knee cyclogram generating model is highly consistent with the original cyclogram.

3.2 Coordination Assessment Results

Data Collection To validate the effectiveness of the hip-knee joint coordination evaluation metric, this study conducted a data collection experiment using the lower limbs motion capture system. A total of ten subjects participated in the experiment, consisting of five hemiplegic individuals (5 males, age: 59.6 ± 8.1 years, height: 173.4 ± 3.1 cm, weight: 79.6 ± 10.4 kg) and five healthy individuals (4 males, 1 female, age: 27.6 ± 4.4 years, height: 172.2 ± 5.0 cm, weight: 64 ± 8.2 kg). All participants were recruited from the Chinese Rehabilitation Research Center.

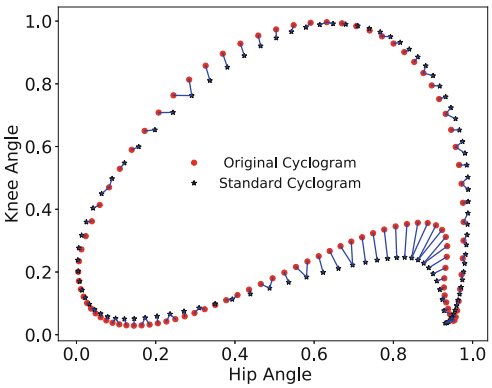

Fig. 8. The visualization of modeling error at the walking speed8. (Color figure online)

An experienced clinician assessed the walking ability of the hemiplegic subjects based on the Brunnstrom Recovery Stage Scale. This study obtained approval from the Ethics Committee of China Rehabilitation Research Center, and all participants provided written informed consent before taking part in the experiment. For the healthy subjects, they walked on a walking machine at a speed that felt comfortable to them while their hip and knee joint kinematics data were recorded for a duration of one minute. To ensure the safety of the hemiplegic subjects, a two-meter force-measuring platform was used for their walking experiment instead of the walking machine. They were instructed to walk at a comfortable speed. Given their limited walking ability, the hemiplegic subjects were asked to perform two walking trials on the force-measuring platform.

Assessment Performance. Clinicians can assess the hip-knee joint coordination of subjects by examining their hip-knee cyclograms. To aid clinicians in distinguishing abnormal gait, this study presents the matching results of corresponding points between each subject's hip-knee cyclogram and the cyclogram generated by the hip-knee cyclogram generation model at a comfortable walking speed. These results are illustrated in Fig. 9.

In Fig. 9, the first two rows show corresponding points matching results of the hip-knee cyclograms from the affected side and the unaffected side of the five hemiplegia subjects (i.e. AHS1-5, UHS1-5), respectively. The last row shows the corresponding point matching results from the right domain leg of the five healthy subjects (i.e. RHS1-5). The blue curves represent the cyclograms from subjects. The red curve represents the standard cyclogram at the normal walking speed. The black solid lines connect the matched corresponding points of the two cyclograms. The curves with $\triangle$ on all cyclograms represent the stance phase of the gait cycle, and the curves with + on all cyclograms represent the swing phase of the gait cycle.

First of all, from the perspective of the hip-knee cyclogram shapes, the hip-knee cyclograms shapes of the healthy subjects are closer to the standard cyclogram and more regular than that of the hemiplegia subjects, especially than the affected side of the hemiplegia subjects. Secondly, from the view of the corresponding points matching degree, the cyclograms of healthy subjects have the best matching effect with the standard cyclograms at the peak points and valley points and also have the largest number of corresponding points. Conversely, the affected side of hemiplegia subjects has the worst matching effect. It shows that the hip-knee joint coordination of healthy subjects is the best, and the worst hip-knee joint coordinations are among hemiplegia subjects.

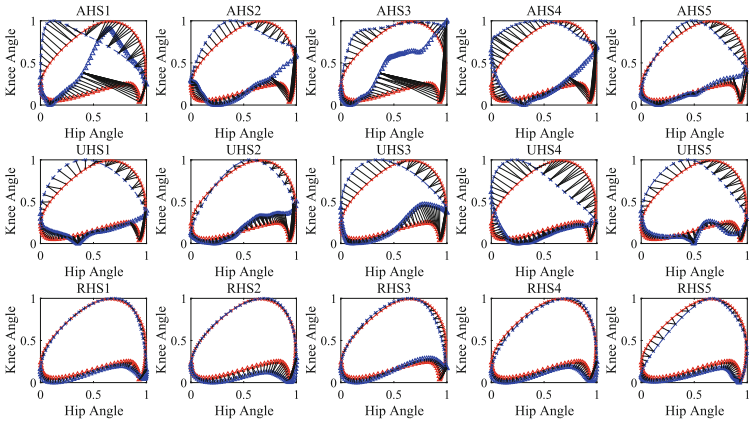

Fig. 9. The qualitative assessment results of the coordination evaluation metric DTW-ED. (Color figure online)

Table 2. Quantitative evaluation results for all subjects

Groups	Leg	Number of subject	DTW-ED	BRS
Hemiplegia	Affect Side	**Subject1**	**0.164 (0.621)**	III
		Subject2	0.161 (0.607)	II
		Subject3	**0.242 (1.000)**	III
		Subject4	0.186 (0.728)	II
		Subject5	0.090 (0.262)	II
Hemiplegia	Unaffect Side	**Subject1**	**0.103 (0.325)**	III
		Subject2	0.111 (0.364)	II
		Subject3	**0.096 (0.291)**	III
		Subject4	0.096 (0.291)	II
		Subject5	0.092 (0.272)	II
Healthy	Right Side	Subject1	0.036 (0.000)	–
		Subject2	0.062 (0.126)	–
		Subject3	0.038 (0.010)	–
		Subject4	0.050 (0.068)	–
		Subject5	0.038 (0.010)	–

[1] the raw result (the min-max normalization result)

Table 2 presents both the raw results and the min-max normalized results of the DTW-ED metric for all subjects. The min-max normalization is applied to facilitate the analysis of the coordination assessment metric's ability to identify abnormal gait. A result closer to zero indicates better hip-knee joint coordination. In Table 2, we can see that the hip-knee joint coordination assessment results of healthy subjects are smaller compared to those of both the affected and unaffected sides of the hemiplegic subjects. With the exception of Hemiplegic Subject 5, the hip-knee joint coordination assessment result for the unaffected side of each hemiplegic subject is smaller than that of their affected side. That is because the unaffected side of Hemiplegic Subject 5 compensates for the affected side, resulting in better hip-knee joint coordination on the affected side. Therefore, the DTW-ED metric for hip-knee joint coordination assessment can not only differentiate between healthy subjects and hemiplegic subjects but also distinguish between the affected and unaffected sides of hemiplegic subjects.

4 Conclusion

This paper introduces a hip-knee joint coordination assessment system. The lower limbs motion capture platform enhances the system's ease of deployment, portability, and cost-effectiveness. The hip-knee cyclogram generation model, utilizing B-spline curve, serves as a reference standard for analyzing abnormal gait patterns. This model provides a more comprehensive understanding of hip-knee joint coordination by considering walking speed. Additionally, the DTW-

ED metric is proposed, enabling both qualitative and quantitative evaluation of hip-knee joint coordination in hemiplegic subjects. This metric combines qualitative observations with quantitative data analysis, improving the comprehensiveness and reliability of hip-knee joint coordination assessment. In conclusion, the hip-knee joint coordination assessment system we proposed by us holds great potential for clinical disease diagnosis.

In future research, we will recruit more subjects with hemiplegia to evaluate the clinical value of the DTW-ED metric. Moreover, we intend to improve the lower limb motion capture system to acquire additional physiological signals, including plantar pressure signals and EMG signals, which will help us study the finer inter-joint coordination assessment model.

References

1. Cicirelli, G., Impedovo, D., Dentamaro, V., Marani, R., Pirlo, G., D'Orazio, T.R.: Human gait analysis in neurodegenerative diseases: a review. IEEE J. Biomed. Health Inf. **26**(1), 229–242 (2022)
2. Wang, W., Ackland, D.C., McClelland, J.A., Webster, K.E., Halgamuge, S.: Assessment of gait characteristics in total knee arthroplasty patients using a hierarchical partial least squares method. IEEE J. Biomed. Health Inf. **22**(1), 205–214 (2018)
3. Ma, H., Zhong, C., Chen, B., Chan, K.M., Liao, W.H.: User-adaptive assistance of assistive knee braces for gait rehabilitation. IEEE Trans. Biomed. Eng. **26**(10), 1994–2005 (2018)
4. Ramirez-Bautista, J.A., Huerta-Ruelas, J.A., Chaparro-Cárdenas, S.L., Hernández-Zavala, A.: A review in detection and monitoring gait disorders using in-shoe plantar measurement systems. IEEE Rev. Biomed. Eng. **10**, 299–309 (2017)
5. Tunca, C., Salur, G., Ersoy, C.: Deep learning for fall risk assessment with inertial sensors: utilizing domain knowledge in spatio-temporal gait parameters. IEEE J. Biomed. Health Inf. **24**(7), 1994–2005 (2020)
6. Saleh, M., Murdoch, G.: In defence of gait analysis observation and measurement in gait assessment. J. Bone Joint Surg. Brit. **67**(2), 237–241 (1985)
7. Gladstone, D.J., Danells, C.J., Black, S.E.: The Fugl-Meyer assessment of motor recovery after stroke: a critical review of its measurement properties. Neurorehabil. Neural Repair **16**(3), 232–240 (2002)
8. Grieve, D.W.: Gait patterns and the speed of walking. Biomed. Eng. **3**(3), 119–122 (1968)
9. Goswami, A.: A new gait parameterization technique by means of cyclogram moments: application to human slope walking. Gait Posture **8**(1), 15–36 (1998)
10. Tepavac, D., Field-Fote, E.C.: Vector coding: a technique for quantification of intersegmental coupling in multicyclic behaviors. J. Appl. Biomech. **17**(3), 259–270 (2001)
11. Hamill, J., Haddad, J.M., McDermott, W.J.: Issues in quantifying variability from a dynamical systems perspective. J. Appl. Biomech. **16**(4), 407–418 (2000)
12. Ryan, C., Emmerik, R.V., Hamill, J.: Quantifying rearfoot-forefoot coordination in human walking. J. Biomech. **41**(14), 3101–3105 (2008)
13. Needham, A.R., Roozbeh, N., Nachiappan, C.: A new coordination pattern classification to assess gait kinematics when utilising a modified vector coding technique. J. Biomech. **48**(12), 3506–3511 (2015)

14. Beitter, J., Kwon, Y.H., Kirsten, T.F.: A combined method for binning coupling angles to define coordination patterns. J. Biomech. **103**, 109598 (2020)
15. Sakoe, H., Chiba, S.: Dynamic programming algorithm optimization for spoken word recognition. IEEE Trans. Acoust. Speech Signal Process. **26**(1), 43–49 (1978)
16. Ren, S., Wang, W., Hou, Z.-G., Chen, B., Liang, X., Wang, J., et al.: Personalized gait trajectory generation based on anthropometric features using random forest. J. Ambient Intell. Hum. Comput. 1–12 (2019)
17. Claudiane, A.F., Reginaldo, F.K., Marcos, D.: A public dataset of overground and treadmill walking kinematics and kinetics in healthy individuals. PeerJ **6**, e4640 (2018)
18. Carl, D.B.: On calculating with B-splines. J. Approx. Theory **6**(1), 50–62 (1972)